Optimum Carburized and Hardened Case Depth

Robert Errichello and Andrew Milburn

Abstract

The optimum carburized and hardened case depth for each gear failure mode is different and must be defined at different locations on the gear tooth. Current gear rating standards do not fully explain the different failure modes and do not clearly define the different locations that must be considered. Furthermore, they use different hardness values to define effective case depth and provide different values for recommended case depth. This paper explains why case hardening is beneficial; the risks involved and compares the methods for calculating and specifying case depth per the ISO 6336-5 and ANSI/AGMA 2101-D04 gear rating standards, and guidelines presented in the MAAG Gear Handbook. The paper shows the three locations that the case depth needs to be specified and presents separate calculation methods to determine the optimum case depth to avoid the failure modes of macropitting, subcase fatigue, bending fatigue, and case/core separation. For each failure mode there is a minimum case depth below which the load capacity drops off. On the other hand, an excessively deep case decreases load capacity, increases cost, and has other detrimental effects that are explained.

Introduction

This paper recommends case depth for carburized gears for the failure modes of macropitting, subcase fatigue, bending fatigue, and case/core separation. See ANSI/AGMA 1010 (Ref. 1) for more information on failure modes. However, the optimum case depth for each failure mode must be defined at different locations on the gear tooth, and the optimum case depth varies with the failure mode. Therefore, this paper discusses required case depth to avoid each failure mode separately considering critical locations for measuring case depth. For more information on the concept of optimum case depth (Refs. 2–3).

Definition of Effective Case Depth

The European definition for effective case depth is the distance from the surface to a point within the case where the hardness is 550 HV (approximately 52.3 HRC). This measurement is done with a Vickers microhardness indenter. The US definition for effective case depth is the distance from the surface to a point within the case where the hardness is 50 HRC (approximately 513 HV). This measurement is done with a Knoop or Vickers indenter, and the hardness values can be converted to HRC using a conversion chart such as ASTM E140.

Maximum grind stock removal must be accounted for when designing case depth to ensure the finished case depth is adequate. Therefore, a typical drawing specification is defined as the effective case depth to 550 HV or 50 HRC after final machining.

Note that the US definition is deeper than the European definition. Unfortunately, there is no easy way to convert between the two definitions because the slope of the hardness gradient varies with the dimensions of the specific gear, material hardenability, and heat treatment process including the quench rate. Consequently, to compare the two definitions, an actual microhardness gradient must be measured on the specific gear to determine how much deeper the 50 HRC case depth is compared to the 550 HV case depth. Some laboratories measure and report both depths to help resolve this issue.

The 550 HV definition for effective case depth is used in this paper because the recommendations for case depth are based on MAAG and ISO guidelines.

Definition of Total Case Depth

The total case depth is approximately 1.5 times and can be as much as twice the effective case depth based on the 550 HV definition. The total case depth is sometimes defined as the depth where the carbon gradient of the case is 0.04% above the core carbon content of the steel alloy.

Recommended Locations for Carburized Case Depth Measurements

Figure 1 shows the authors' recommended locations for case depth measurements and is based on Dudley's (Ref. 4, Fig. 4.8). The 30° line was added to define the location for case depth measurement at the root fillet.

- Location A, at approximately mid-height of the tooth, is the location for measuring case depth at the flank.

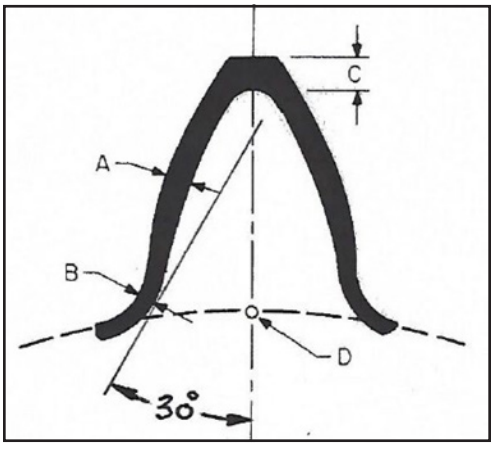

Figure 1 Locations for carburized case depth measurements.

- Location B is the location for measuring case depth at the root fillet.
- Location C is the location for measuring case depth at the tooth tip.
- Location D, on the root circle, is the location for measuring core hardness.

Another aspect besides failure mode that must be considered when specifying case depth is the fact that case depth can be different at the flank, root, and tip locations. Atmosphere carburizing produces case depths that depend on several factors including material hardenability, gear tooth geometry, furnace parameters, and quenching parameters, hence the variation between flank, root, and tip case depths varies widely; sometimes the same, sometimes quite different. Typically, the case depth will be less at the root than at the flank and less at the flank than at the tip locations. In contrast, vacuum carburizing can produce a nearly uniform case depth at every location.

Influence of Case Depth on Gear Tooth Properties

Benefits of carburizing. Carburized gear teeth have maximum macropitting and bending fatigue resistance because they have hard surfaces, and carburizing induces beneficial compressive residual stresses in the case. The compressive residual stresses are the result of the material expansion when austenite transforms to martensite and they effectively lower load stresses. However, the compressive residual stresses in the case are balanced by detrimental tensile residual stresses near the case/core boundary as shown (Fig. 2).

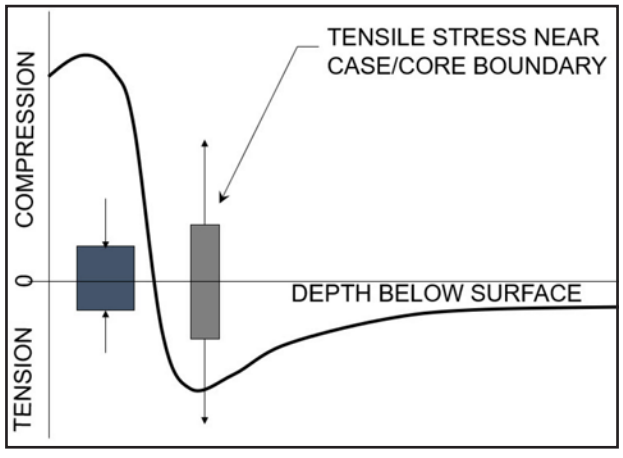

Figure 2 Residual stresses in carburized gears.

Optimum case depth. Generally, for each failure mode there is a minimum case depth below which the load capacity drops off (Refs. 2–3). On the other hand, an excessively deep case decreases load capacity (Refs. 2–3). Furthermore, deep cases require long carburizing times, which is undesirable for the following reasons:

- Intergranular oxidation (IGO) increases (especially with alloys containing Mn, Cr, and Si), which decreases bending fatigue resistance.
- Residual stress profiles are altered, which is especially detrimental because beneficial compressive residual stresses decrease, and both Hertzian fatigue resistance and bending fatigue resistance decrease.
- Grain size might increase, which decreases both Hertzian fatigue resistance and bending fatigue resistance.
- Excessively deep cases promote case/core separation.
- Distortion increases, which requires greater grind stock removal.
- Manufacturing costs might increase.

Macropitting

Macropitting might initiate at the tooth surface or at a shallow depth below the surface usually at a subsurface defect such as a nonmetallic inclusion. It is important to design the effective case depth to achieve high compressive residual stresses at the surface and within the case to mitigate the influence of nonmetallic inclusions. Table 1 gives several guidelines for minimum effective case depth to avoid macropitting.

Table 1 Different guidelines for minimum case depth to avoid macropitting

Reference No.	Source	Location	Material Grade	Note No.
5	MAAG	Fig. 6.12	---	1, 3
6	ISO 6336-5	Clause 5.6.2.a	ML, MQ, ME	1, 3
7	AGMA 2101-D04	Fig. 13	1, 2, 3	2, 3

1. Effective case depth is based on the 550 HV definition.
2. Effective case depth is based on the 50 HRC definition.
3. See Annex A for equations.

Macropitting recommendation. Figure 3 shows the authors' recommended effective case depth based on the MAAG (Ref. 5). See Annex B for the derivation of Figure 3 and a comparison to the ISO 6336-5 (Ref. 6) and ANSI/AGMA 2101 (Ref. 7) guidelines.

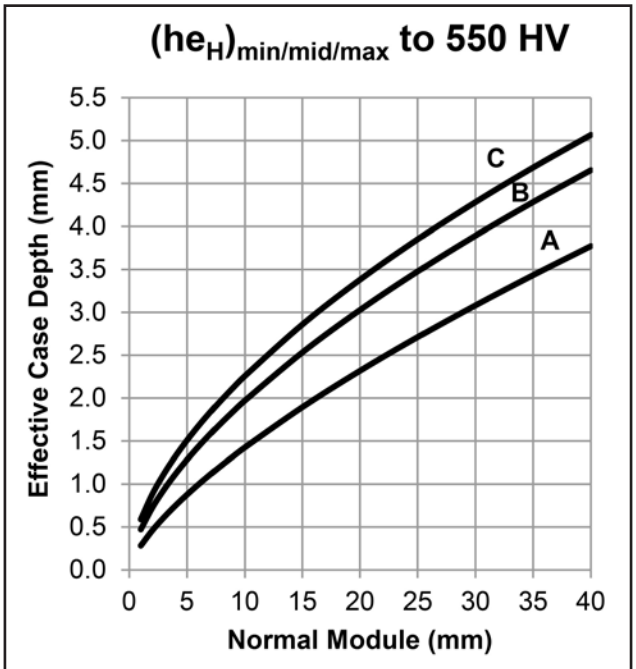

Figure 3 Effective case depth to avoid macropitting, $(he_H)_{min/mid/max.}$

Description of Figure 3. The lower curve "A" in Figure 3 is the minimum effective case depth measured at location A shown (Fig. 1). It is the case depth after all machining is complete and is the distance measured from the tooth flank surface to a depth where the hardness is 550 HV. Curve "A" is recommended for maximum macropitting resistance. However, the designer should provide a tolerance for case depth to accommodate manufacturing variation. The tolerance band width usually depends on the type of gear unit, the conditions imposed on it, the

facilities in the heat treat shop, and the uniformity of the heat treat results. Curves "B" and "C" are tolerance bands for maximum case depth obtained by adding a tolerance to the minimum effective case depth represented by curve "A". Curve "C" represents the maximum tolerance range customary in commercial gear drive design. Curve "B" is appropriate for the tolerance range for a precision gear drive design.

***Equations for Figure 3 curves*:**

Curve A $(he_H)_{min} = 0.2835(m_n)^{0.7016}$ (minimum to avoid macropitting)

Curve B $(he_H)_{mid} = 0.4730(m_n)^{0.6198}$ (maximum precision tolerance)

Curve C $(he_H)_{max} = 0.5899(m_n)^{0.5829}$ (maximum commercial tolerance)

Subcase Fatigue

The term "case crushing" was incorrectly used in earlier gear nomenclature for subcase fatigue. However, subcase fatigue is now the preferred term. See ANSI/AGMA 1010 (Ref. 1) for more information.

Case depth, Hertzian stress, residual stress, and material fatigue strength influence subcase fatigue. The subsurface distribution of residual stresses and fatigue strength depends on case hardness, case depth, and core hardness. Optimum values of case depth and core hardness give proper balance of residual stresses and fatigue strength to maximize subcase fatigue resistance (Refs. 2–3).

To prevent subcase fatigue, the steel alloy must have adequate hardenability to obtain optimum case and core properties. Furthermore, it is especially important to use clean steel because inclusions can initiate fatigue cracks if they occur near the case/core interface in areas of tensile residual stress (Fig. 2).

Overheating gear teeth during operation or manufacturing (such as grind temper) can lower case hardness, alter residual stresses, and reduce resistance to subcase fatigue. In fact, grind temper is often the root cause of subcase fatigue failure.

Table 2 gives guidelines for minimum effective case depth to avoid subcase fatigue.

Table 2 Different guidelines for minimum case depth to avoid subcase fatigue

Reference No.	Source	Location	Material Grade	Note No.
6	ISO 6336-5	Clause 5.6.2.c	ML, MQ, ME	1
7	AGMA 2101-D04	Eq. 43	1, 2, 3	2

1. Clause 5.6.2.c has $U_H = 66{,}000$ N/mm2 for grades MQ and ME, which is based on case depth = 2.1 times the depth to the maximum shear stress, and $U_H = 44{,}000$ N/mm^2 for grades ML, which is based on case depth = 3.2 times the depth to the maximum shear stress.
2. Eq. 43 has $U_H = 44{,}000$ N/mm^2, which is based on case depth = 3.2 times the depth to the maximum shear stress.

Subcase fatigue recommendation. It is the authors' opinion that the AGMA guideline is too deep for the reasons given previously (for more information see References 2 and 3). Therefore, it is recommended that the ISO 6336-5 (Ref. 6) equation in clause 5.6.2.c be used, which is given in Annex A and repeated here as Equation 1 for convenience.

$$(he_s)_{min} = \left\{ \frac{\sigma_H d_{w1} \cdot sin(\alpha_{wt})}{U_H \times cos(\beta_b)} \right\} \cdot C_G \quad (1)$$

Where $U_H = 66{,}000$ MPa for ISO quality grades MQ and ME (AGMA grades 2 and 3) and $U_H = 44{,}000$ MPa for quality grade ML (AGMA grade 1). Note that Equation 1 is based on the 550 HV definition of case depth and is for the flank (location A).

The Hertzian stress σ_H should equal the maximum stress actually applied in service. For applications with heavy shock loads, the required minimum effective case depth can be significantly higher than that shown by curve A (Fig. 3). Therefore, σ_H must be carefully chosen because an excessively deep case will decrease both macropitting resistance and bending fatigue resistance. This requires an analysis of the subsurface gradients of strength, residual stresses, and Hertzian stresses due to applied loads.

Figure 4 shows the effective case depth based on the recommended subcase fatigue criteria at two different contact stress numbers and additional lines, which have been added for reference. The gear geometry used for the subcase fatigue calculations is shown (Table 3). The AGMA heavy line was multiplied by 0.9 to adjust it from the 50 HRC definition to the 550 HV definition of case depth.

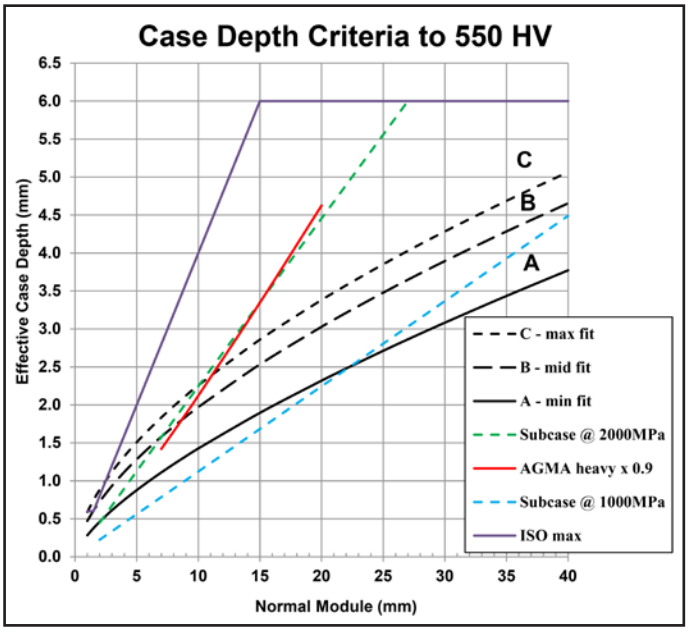

Figure 4 Effective case depth based on subcase fatigue criteria at two different contact stress numbers.

Table 3 shows the gear set geometry used to calculate the subcase effective case depth data points in Figure 4 and the maximum effective case depth data points using pinion topland thickness in Figure 7.

Bending Fatigue

Case hardening by carburizing is especially beneficial because carburizing induces compressive residual stresses that reduce net tensile bending stresses. In addition, shot peening can be used to enhance the compressive residual stresses at the surfaces of the root fillets. For carburized gears there are optimum values of case hardness, case depth, and core hardness that give the proper balance of residual stresses and fatigue strength to maximize resistance to bending fatigue (Refs. 1–3). Note that the optimum case depth to avoid bending fatigue is less than the optimum case depth to avoid macropitting. Therefore, it is important to measure the root case depth in addition to the flank case depth. Table 4 gives several guidelines for minimum effective case depth to avoid bending fatigue.

Bending fatigue recommendation. Figure 5 shows the authors' recommended minimum effective case depth to avoid bending fatigue. See Annex C for the derivation of Figure 5 and a comparison to ISO 6336-5 (Ref. 6) guideline for optimum case depth to avoid bending fatigue.

***Equation for Figure 5 curve*:**

$$(he_F)_{min} = 0.2016\ (m_n)^{0.7994} \quad (2)$$

Table 3 Gear data used for subcase fatigue and tooth tip thickness calculations

Module	mm	2		10		40	
Center Distance	mm	98		500		2,000	
Reference Pressure Angle	Degrees	20		20		20	
Operating Pressure Angle	Degrees	22.942		22.942		22.942	
Cutter Addendum		1.4×Module		1.4×Module		1.4×Module	
Cutter Tip Radius		0.3×Module		0.3×Module		0.3×Module	
		Pinion	Gear	Pinion	Gear	Pinion	Gear
Number of Teeth		25	73	25	73	25	73
Profile Shift Coefficient		0.516	0.556	0.516	0.556	0.516	0.556
Operating Pitch Diameter	mm	51.02	148.98	255.10	744.90	1,020.4	2,979.5
Tip Diameter	mm	55.91	152.09	279.60	760.40	1,118.4	3,041.6
Tooth Thickness at Tip	mm	1.12	1.46	5.56	7.30	22.29	29.18
AGMA Pitting Geometry Factor		0.127		0.127		0.127	
AGMA Bending Geometry Factor		0.457	0.421	0.440	0.421	0.433	0.421

Table 4 Different guidelines for minimum case depth at root fillet to avoid bending fatigue

Reference No.	Source	Location	Material Grade	Note No.
4	Dudley	Eq. 4.2a	1, 2, 3	1
6	ISO 6336-5	Clause 5.6.2.b	ML, MQ, ME	2
7	AGMA 2101-D04	Table 9	2, 3	3

1. Reference 4 recommends a case depth of 0.16(m_n) at position B on the root fillet (Fig. 1).
2. Reference 6 states: "The optimum effective case depth relating to permissible bending stress for long life at the root fillet on a normal to the 30° $_{tangent}$ after tooth finishing: 0.1–0.2(m_n)."
3. Reference 7 recommends 50% of minimum specified case depth at 1/2 tooth height for grade 2, and 66% for grade 3.

Subsurface-Initiated Bending Fatigue

Classic bending fatigue failures initiate at the surface of the root fillet on the tensile side of the gear tooth. However, when a bending fatigue crack initiates at a location significantly above the root fillet, where the nominal bending stress is much lower than at the root fillet, it is likely that the root cause of failure is a material flaw, such as a nonmetallic inclusion. Hard un-deformable inclusions such as calcium aluminate have a lower thermal expansion coefficient than steel and they develop tensile residual stresses concentrated around each inclusion as a result of hardening heat treatments. The tensile residual stresses from the inclusions and the existing tensile residual stresses below the case/core boundary add to the nominal bending stress from the applied load. Therefore, a nonmetallic inclusion can shift the location of the crack origin from the surface of the root fillet to below the case/core boundary or other areas. Consequently, nonmetallic inclusions are often the root cause of bending fatigue cracks that initiate at a subsurface location below the case/core boundary. Typically, the crack initiates at a nonmetallic inclusion that is located at a depth of approximately 2.5 times the depth of the effective case depth in an area of high tensile residual stress (Fig. 2). The deeper the effective case depth is the further from the surface the potentially damaging tensile residual stress peak. This relationship, along with the fact that applied stresses diminish with distance from the surface, reduces the chances of a fatigue failure initiating near the core/core boundary. Currently, there is no industrial standard for assessing the risk of subsurface-initiated bending fatigue. However, ISO/DTS 6336-4 (Ref. 8) is a draft technical specification that is currently under development to address the failure mode.

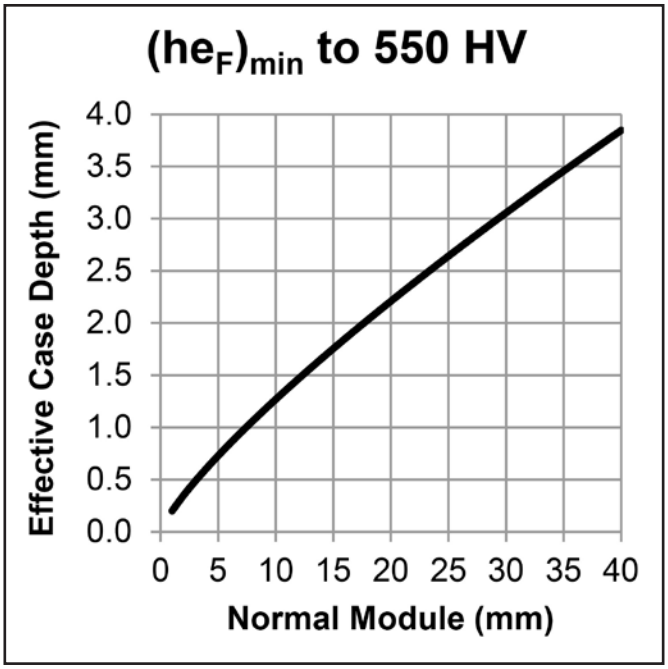

Figure 5 Effective case depth to avoid bending fatigue *$(he_F)min$*.

Case/Core Separation

Figure 6 shows a case/core crack that occurred in a carburized gear tooth below the case/core interface near the tip of the tooth. Case/core separation occurs when compressive residual stresses in the case exceed the tensile strength in the core near the tooth tip due to excessive case depth at the tip. Internal cracks can propagate causing corners, edges, or entire tips of teeth to separate. Cracks can appear immediately after heat treatment, during subsequent handling or storage, or after time in service.

If tensile residual stress is high and ductility is low, brittle fracture can occur and tips of teeth can separate explosively. If conditions are less severe, cracks might arrest before reaching tooth

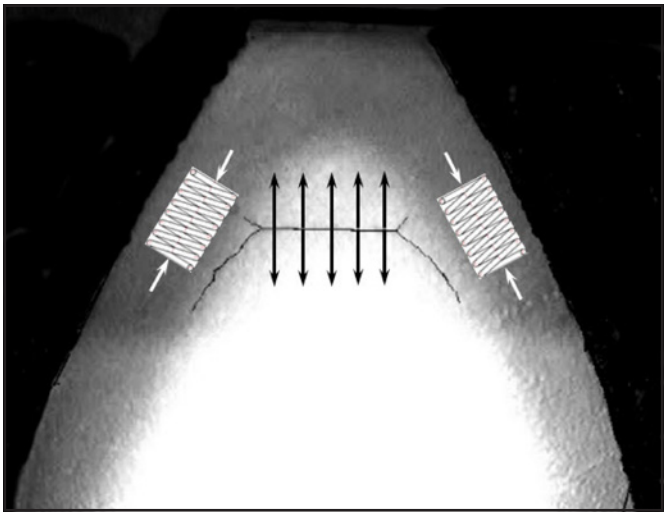

Figure 6 Image of case/core separation crack and arrows showing location of residual compressive and tensile stresses.

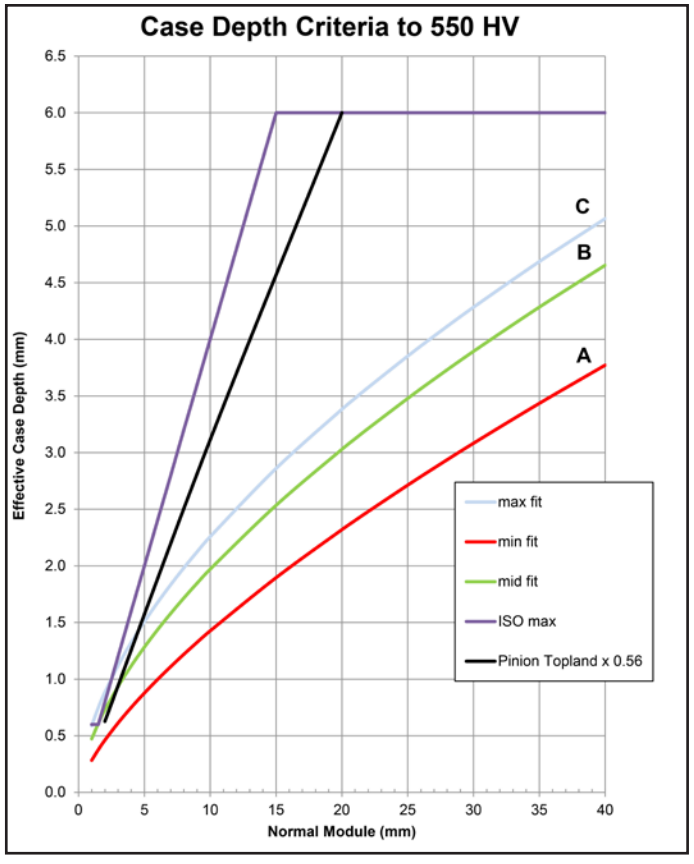

Figure 7 Black line shows maximum effective case depth based on 0.56 times the pinion topland width for the example gear sets.

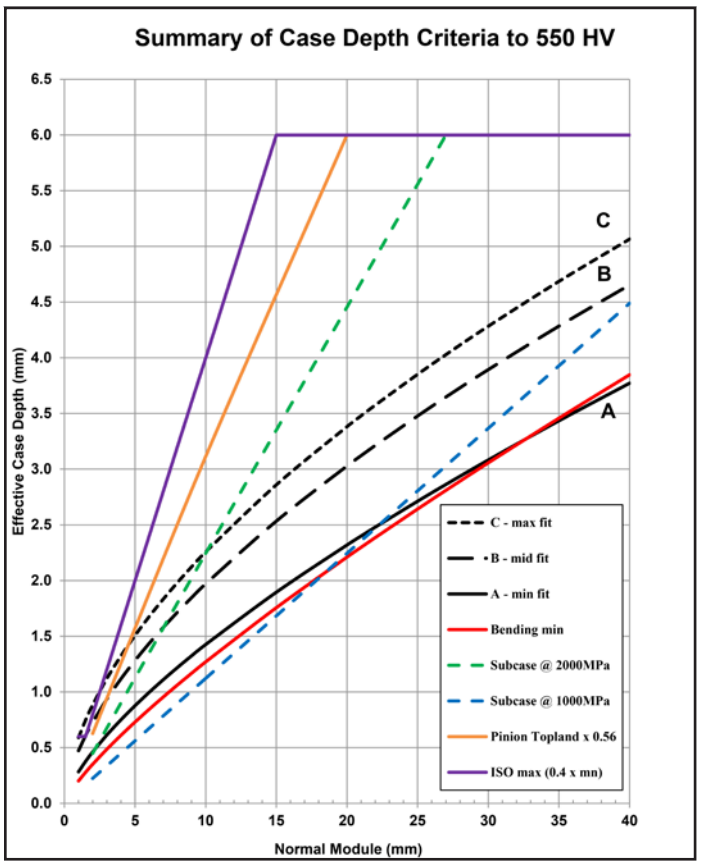

Figure 8 Summary plot showing recommended effective case depth for four different failure modes.

surfaces. Inclusions promote case/core separation — especially when they occur near the case/core interface in areas of tensile residual stress (Fig. 2). Hydrogen can accumulate at inclusions and cause brittle fracture. Stresses in service can cause cracks to grow by fatigue. The risk of case/core separation can be reduced by avoiding narrow toplands or masking toplands with copper plate to restrict carbon penetration during carburizing to prevent overly deep cases.

Case/core separation is a brittle fracture. Therefore, to avoid case/core separation, it is important to ensure the material has high fracture toughness. The best toughness properties are obtained with 3%NiCrMo steels with core hardness in the range of 30–40 HRC. Toughness can be maximized by using vacuum-melted steel and keeping carbon, phosphorus, and sulfur content as low as possible. See AGMA 1010 (Ref. 1) for more information.

Table 5 gives several guidelines for maximum effective case depth to avoid case/core separation. Unfortunately, there are conflicts between ISO 6336 (Ref. 6) and AGMA 2101 (Ref. 7), which both allow $0.4(m_n)$ maximum effective case depth at the tooth flank, whereas Dudley (Ref. 4) and AGMA 911 (Ref. 9) recommend $0.4(m_n)$ maximum effective case depth at the tooth tip.

Table 5 Different guidelines for maximum case depth at tooth tip to avoid case/core separation

Reference No.	Source	Location	Material Grade	Note No.
4	Dudley	Eq. 4.4a	1, 2, 3	1
6	ISO 6336-5	Clause 5.6.2.d	ML, MQ, ME	2
7	AGMA 2101-D04	Eq. 44	2, 3	3
9	AGMA 911-A94	Clause 9.12	1, 2, 3	4

1. Reference 4 recommends a maximum effective case depth of 0.40(m_n) at position C at the tooth tip (Fig. 1).
2. Reference 6 allows a maximum effective case depth of 0.4(m_n) at position A at the mid-height of the tooth or 6 mm maximum.
3. Reference 7 allows a maximum effective case depth of 0.4(m_n) at position A at the mid-height of the tooth or 56% of the normal topland tooth thickness — whichever is less.
4. Reference 9 states: "The case must not be so great as to result in brittle teeth tips and edges, or high residual tensile stresses in the core. Maximum case depth at the tooth tip should be limited to 56% of the tooth topland thickness."

Case/core separation recommendation. The case depth at the tooth tip is critical for the case/core separation failure mode. Therefore, the authors recommend that the maximum effective case depth to 550 HV at the tooth tip (position C in Figure 1) be limited to $(he_T)max = 0.40(m_n)$ or 56% of the topland thickness — whichever is less.

Figure 7 shows a line based on the criteria of 0.56 times the pinion tip thickness. Note that this criterion is now based on a depth to 550 HV whereas the current AGMA 2101 uses the same criteria based on a depth to 50 HRC. Calculations were made for three different gear sets with the geometry summarized in Table 3.

Figure 8 is a summary plot that shows recommended case depths for all four failure modes discussed in this paper.

Conclusions

1. Since the effective case depth can vary depending on where it is measured, the authors recommend it be specified at three different locations (Fig. 1).
2. The optimum case depth at each location depends on the failure mode being considered.
3. The paper compares case depth guidelines from several different sources and presents the author's recommendations for four different failure modes.

Annex A: Equations for Effective Case Depth Nomenclature for Equations:

Root nomenclature:

$(h_{eF})_{min}$ = AGMA root minimum effective case depth to 50 HRC after finishing based on bending fatigue.

$(h_{eF})_{min}$ = Dudley root minimum effective case depth to 50 HRC after finishing based on bending fatigue.

$(h_{eF})_{min}$ = MAAG root minimum effective case depth to 550 HV after finishing based on bending fatigue.

$(h_{eF})_{opt}$ = ISO root optimum effective case depth to 550 HV after finishing based on bending fatigue.

Flank nomenclature:

$(h_{eH})_{max}$ = MAAG flank maximum (commercial tolerance) effective case depth to 550 HV after finishing based on macropitting.

$(h_{eH})_{mid}$= MAAG flank maximum (precision tolerance) effective case depth to 550 HV after finishing based on macropitting.

$(h_{eH})_{min}$ = AGMA flank minimum effective case depth to 50 HRC after finishing based on macropitting (normal and heavy case depths).

$(h_{eH})_{min}$ = MAAG flank minimum effective case depth to 550 HV after finishing based on macropitting.

$(h_{eH})_{opt}$ = ISO flank optimum effective case depth to 550 HV after finishing based on macropitting.

$(h_{eS})_{min}$ = AGMA flank minimum effective case depth to 50 HRC after finishing based on subcase fatigue.

$(h_{eS})_{min}$ = ISO flank minimum effective case depth to 550 HV after finishing based on subcase fatigue.

Tip nomenclature:

$(h_{eT})_{max}$ = AGMA tip maximum effective case depth to 50 HRC after finishing based on case/core separation.

$(h_{eT})_{max}$ = Dudley tip maximum effective case depth to 50 HRC after finishing based on case/core separation.

Equations for Flank Case Depth

AGMA 2101 (Ref. 7) Figure 13 (flank 50 HRC):

Normal case depth

$(he_H)_{min} = 3.046349\,(25.4/m_n)^{-0.86105} = 0.1880\,(m_n)^{0.8611}$

Heavy case depth

AGMA 2101 (Ref. 7) Based on Subcase Fatigue Eq (43) where U_H = 44,000 MPa:

$(he_S)_{min} = [\sigma_H d_{w1} sin(\alpha_{wt})/U_H cos(\beta_b)]C_G$

ISO 6336-5 (Ref. 6) Figure 17 Optimum Case Depth (flank 550 HV):

$(he_H)_{opt} = CHD_{H,opt} = 0.15\,(m_n)$ for module range $2 \le m_n \le 10$

$(he_H)_{opt} = CHD_{H,opt} = 0.083(m_n) + 0.67$ for module range $10 < m_n \le 40$

ISO 6336-5 (Ref. 6) Based on Subcase Fatigue Clause (5.6.2.c) where U_H=66,000 MPa for Quality Grades MQ/ME and U_H=44,000 MPa for Quality Grade ML (flank 550 HV):

$(he_S)_{min} = [\sigma_H d_{w1} sin(\alpha_{wt})/U_H cos(\beta_b)]C_G$

MAAG (Ref. 5) Empirical Formula Clause (6.422) (flank 550 HV):

$(he_H)_{min} = (m_n/2 + 1.1)^{½} - 1$

Equations of Curves Fitted to MAAG (Ref. 5) Figure 6.12 (see Annex B) (flank 550 HV):

$(he_H)_{min} = 0.2835(m_n)^{0.7016}$ (minimum to avoid macropitting)

$(he_H)_{mid} = 0.4730(m_n)^{0.6198}$ (maximum precision tolerance)

$(he_H)_{max} = 0.5899(m_n)^{0.5829}$ (maximum commercial tolerance)

Equations for Root Case Depth

AGMA 2101 (Ref. 7) Table 9 (root 50 HRC):

$(he_F)_{min} = 0.50\,(he_H)_{min}$ for grade 2

$(he_F)_{min} = 0.66\,(he_H)_{min}$ for grade 3

ISO 6336-5 (Ref. 6) Optimum Case Depth Clause (5.6.2.b) (root 550 HV):

$(he_F)_{opt} = CHD_{F,opt} = 0.10\,(m_n)$ *to* $0.20\,(m_n)$

Dudley (Ref. 4) Optimum Case Depth Eq. (4.2.a) (root 50 HRC):

$(he_F)_{min} = 0.16\,(m_n)$

MAAG Minimum Case Depth to Avoid Bending Fatigue (see Annex C) (root 550 HV):

$(he_F)_{min} = 0.2016\,(m_n)^{0.7994}$

Equations for Tip Case Depth

Dudley (Ref. 4) Maximum Case Depth Eq. (4.4.a) (tip 50 HRC):

$(he_T)_{max} = 0.4\,(m_n)$

ISO 6336-5 (Ref. 6) Maximum Case Depth Clause (5.6.2.d) (flank 550 HV):

$(he_T)_{max} = CHD_{max} = 0.4\,(m_n)\,(\le 6\,mm)$

AGMA 2101 (Ref. 7) Maximum Case Depth Eq. (44) (flank 50 HRC):

$(he_T)_{max}$ = the lesser of $0.4\,(m_n)$ *or* $0.56\,(t_{no})$

Annex B: Derivation of Figure 3

MAAG Guidelines. Figure B-1 shows the original MAAG [5] Figure 6.12.

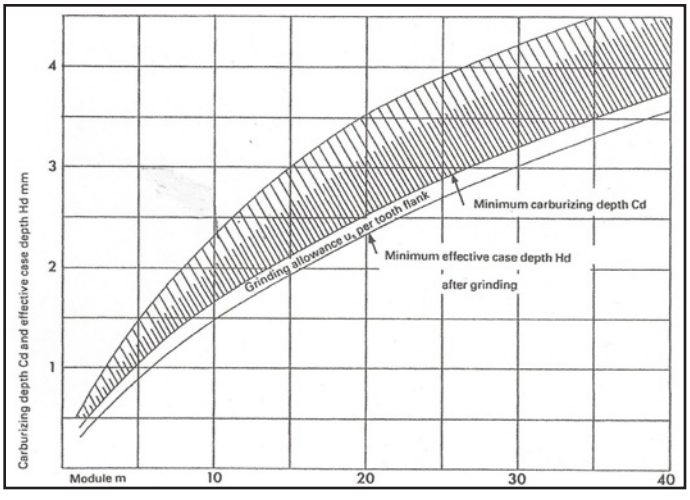

Figure B-1 MAAG Figure 6.12.

Method Used to Derive Figure 3. The following text and Figure B-2 explain the methodology used to derive Figure 3 of this report.

- The lower green line in Figure B-2 conforms to the MAAG (Ref. 5) equation: $(he_H)_{min} = (m_n/2 + 1.1)^{½} - 1$
- The lower red line is an *Excel* power curve fit of the MAAG equation, redefined here as MAAG_min_fit.
- The upper green line and the middle blue line were obtained from the upper and middle curves in MAAG (Ref. 5) Figure 6.12. Values were manually read from Figure 6.12 since no equations were given for these two lines.
- The upper red line and the middle black line are *Excel* power curve fits of the upper green line and middle blue line respectively.
- The lower blue line represents the difference between the upper and lower green lines. Note that the lower blue line does not steadily increase with increasing module. This inspired the *Excel* power curve fits to smooth the final upper and lower red

lines.
- The purple line represents the difference between the upper and lower red lines. Note that the purple line steadily increases with increasing module.

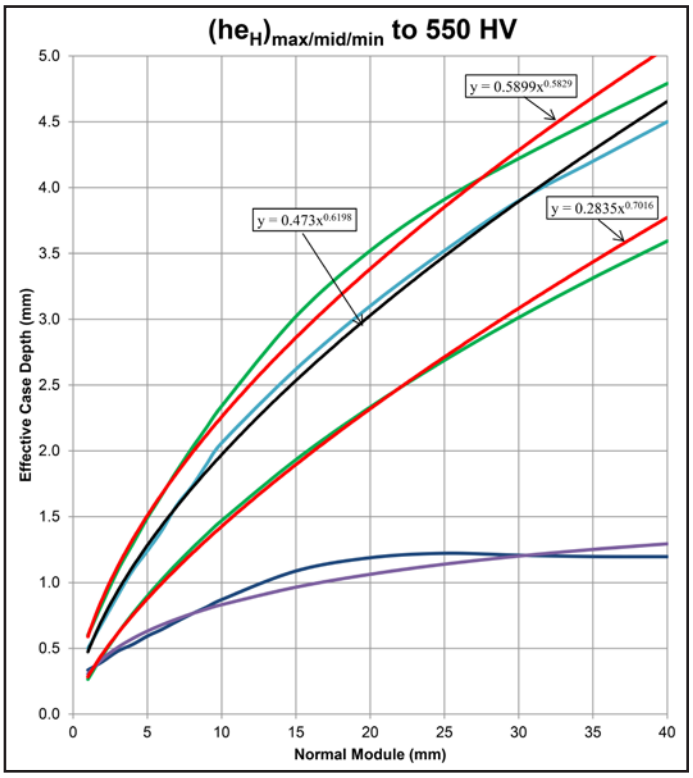

Figure B-2 Derivation of Figure 3.

Comparison of MAAG, ISO 6336-5, and AGMA Guidelines. Figure B-3 compares the $MAAG_{min\_fit}$ (Ref. 5) (black line) and ISO 6336-5 (Ref. 6) optimum (red line) guidelines for minimum effective case depth to 550 HV to avoid macropitting. The MAAG guideline has a long history of successful application. Figure B-3 shows that the $MAAG_{min\_fit}$ and ISO guidelines are very similar over the range of 8–25 normal modules. For modules less than 8, the $MAAG_{min\_fit}$ guideline recommends deeper case depths, and for modules greater than 25 the ISO guideline recommends deeper case depths. Also included are the AGMA normal case depth (blue lines), heavy case depth (green lines), and ISO maximum lines (purple lines). The solid blue and green lines were obtained by multiplying the dashed blue and green lines by 0.9 to adjust the AGMA guidelines from the 50 HRC definition to the 550 HV definition of case depth. It is obvious that the AGMA 2101 Heavy guideline is significantly deeper than $MAAG_{max\_fit}$ tolerance range for modules greater than 10, whereas the AGMA 2101 Normal guideline is similar to the $MAAG_{min\_fit}$ guideline for maximum macropitting resistance, considering that the 50 HRC case depth is deeper than the 550 HV case depth. Note that without data on actual hardness gradients it is not possible to accurately compare case depths based on the 50 HRC definition with the 550 HV definition. Therefore, the comparisons shown in Figure B-3 are only qualitative.

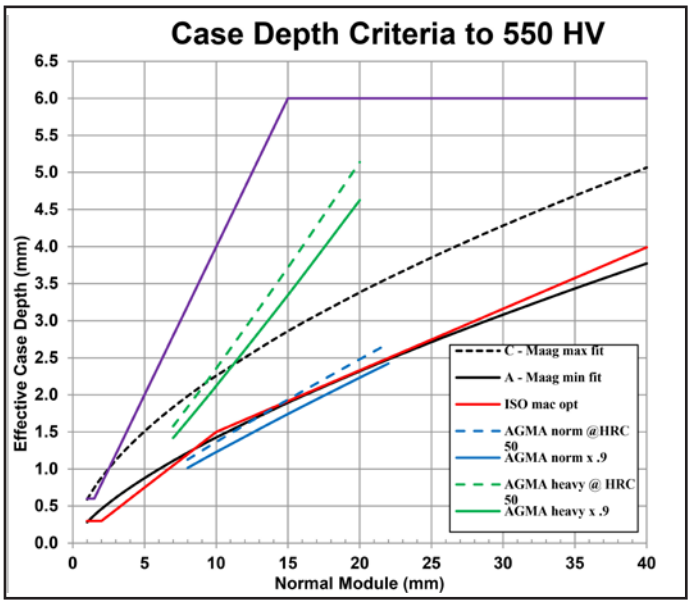

Figure B-3 Comparison of MAAG, ISO, and AGMA flank case depths

Annex C: Derivation of Figure 5

Method used to derive Figure 5 for maximum bending fatigue resistance. The following text and Figures C-1 and C-2 explain the methodology used to derive Figure 5. The lines shown in Figure C-1 are as follows:
- The upper line conforms to the ISO equation $(he_F)_{opt} = 0.2\,(m_n)$ for maximum case depth for bending fatigue resistance.
- The next line down conforms to the MAAG min case depth for maximum macropitting resistance $(he_F)_{min} = 0.2835\,(m_n)^{0.7016}$.
- The red line is the case depth for maximum bending fatigue resistance defined by the equation $(he_H)_{min} = 0.2016\,(m_n)^{0.7994}$. This line was chosen to be slightly lower than the MAAG min case\depth for maximum macropitting resistance and within the ISO limits of $0.1\,(m_n) \le (he_F)_{opt} \le 0.2\,(m_n)$ for maximum bending fatigue resistance.
- The line below the red line conforms to the ISO equation $(he_F)_{opt} = 0.1\,(m_n)$ for minimum case depth for bending fatigue resistance.
- The two lower lines conform to the AGMA 2101 equations for minimum case depth for bending fatigue resistance:
  - $(he_F)_{min} = 0.50\,(he_H)_{min}$ (50% of MAAG min fit) for grade 2
  - $(he_F)_{min} = 0.66\,(he_H)_{min}$ (66% of MAAG min fit) for grade 3

Figure C-2 is an enlarged view of Figure C-1 for $m_n \le 10$. It shows that the equation $(he_F)_{min} = 0.2016\,(m_n)^{0.7994}$ for maximum bending fatigue resistance gives a case depth that is about midway between the ISO limits of $0.1\,(m_n) \le (he_F)_{opt} \le 0.2\,(m_n)$.

References

1. AGMA, 2014. "*Appearance of Gear Teeth - Terminology of Wear and Failure*," ANSI/AGMA 1010- F14.
2. Parrish, G. 1999, *Carburizing: Microstructure and Properties*, ASM International, Materials Park, OH.
3. Doane, D.V. 1990, *Modern Carburized Nickel Alloy Steels*, Nickel Development Institute, Toronto, Ontario, Canada.
4. Dudley, D.W. 1984, *Handbook of Practical Gear Design*, McGraw-Hill, New York, NY.
5. 1990, *MAAG GEAR BOOK*. MAAG Gear Company, Zurich, Switzerland.
6. ISO, 2015. "*Calculation of Load Capacity of Spur and Helical Gears — Part 5: Strength and Quality of Materials*," ISO 6336-5.
7. AGMA, 2004. "*Fundamental Rating Factors and Calculation Methods for Involute Spur and Helical Gear Teeth*," ANSI/AGMA 2101-D04.
8. ISO, 2017. "*Calculation of Load Capacity of Spur and Helical Gears — Part 4: Calculation of Tooth Flank Fracture Load Capacity*," ISO/DTS 6336-4.
9. AGMA, 1994. "*Design Guidelines for Aerospace Gearing*," AGMA 911-A94.

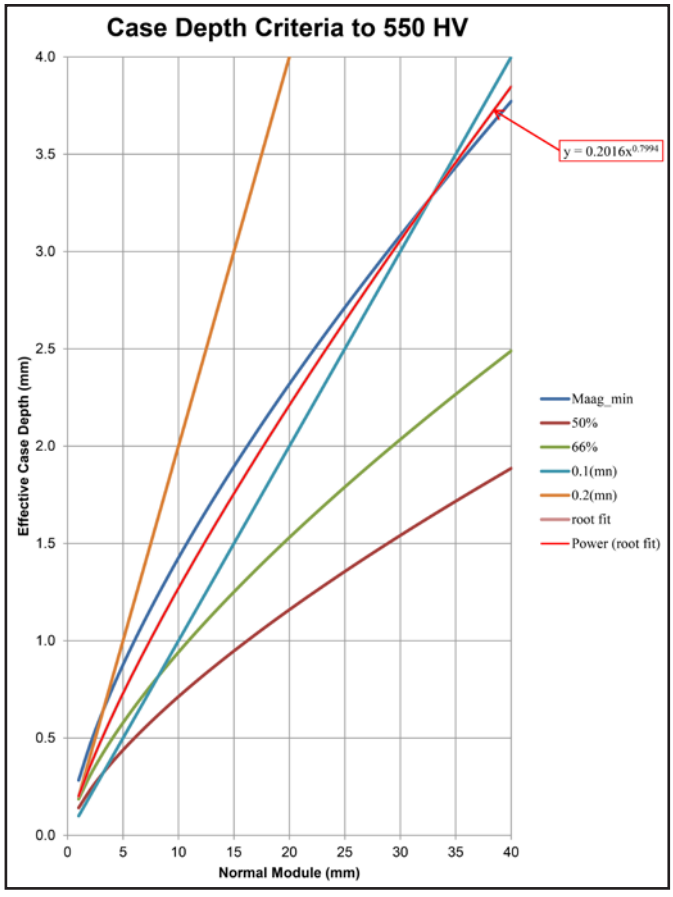

Figure C-1 Derivation of Figure 5.

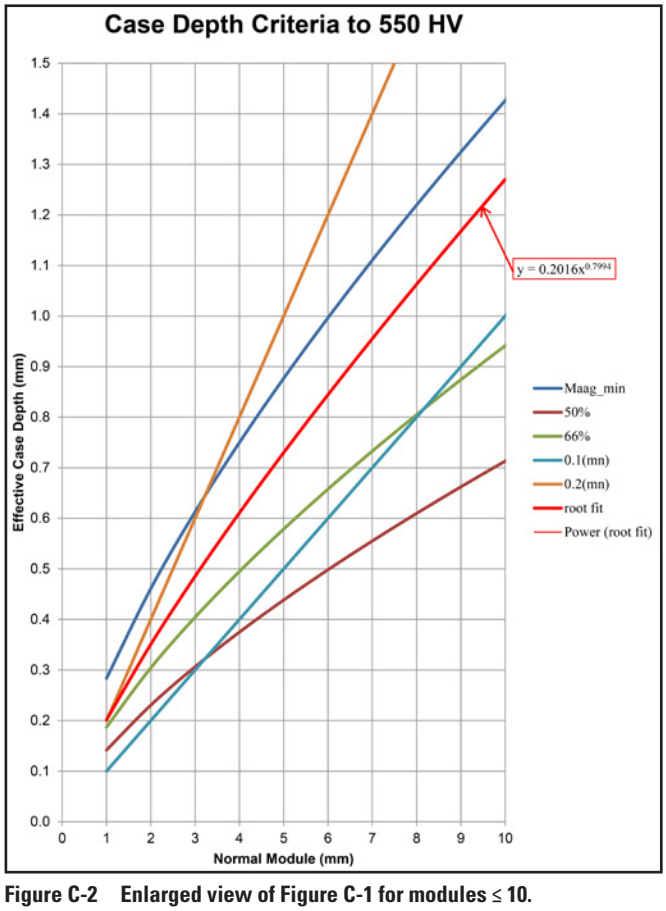

Figure C-2 Enlarged view of Figure C-1 for modules ≤ 10.

Robert Errichello, PE, heads his own gear consulting firm — GEARTECH — and is a founder of GEARTECH Software, Inc. A graduate of the University of California at Berkeley, he holds B.S. and M.S. degrees in mechanical engineering and a master of engineering degree in structural dynamics. In his more than 50 years of industrial experience, Errichello worked for several gear companies; he has also been a consultant to the gear industry for more than 40 years and has taught courses in material science, fracture mechanics, vibration and machine design at San Francisco State University and the University of California at Berkeley. He is also a member of ASM International, STLE, ASME Power Transmission and Gearing Committee, AGMA Gear Rating Committee and the AGMA/AWEA Wind Turbine Committee. Errichello has published over 100 articles on design, analysis and the application of gears, and is the author of three widely used computer programs for the design and analysis of gears. He is also a longtime technical editor for Gear Technology magazine and STLE Tribology Transactions, and has presented numerous seminars on design, analysis, lubrication and failure analysis of gears. Errichello is a past recipient of the AGMA TDEC award, the STLE Wilbur Deutch Memorial award, the AGMA Lifetime Achievement Award, the E.P. Connell Award and the STLE Bisson Award.

Andy Milburn is currently president of Milburn Engineering, Inc., a consulting firm located near Tacoma, Washington and has 45 years experience in the design and analysis of gears and gearboxes. Prior to starting his own consulting firm in 1989 he worked at The Gear Works in Seattle, WA for 15 years and was involved in all aspects of gear manufacturing, gear failure analysis and designed many custom industrial gearboxes. As a consultant he has investigated numerous gear and bearing failures, and helped clients improve their gear products. During the past 18 years he has been very active in the wind industry investigating gearbox failures, developing gearbox modifications and participating in due diligence design reviews. He was a U.S. delegate to ISO TC66, working on the new international gearbox standard, IEC 81400-4. He is a registered Professional Engineer in the state of Washington, a member of AGMA, ASME, ASM and STLE and a member of the AGMA Helical Gear Rating Committee. Milburn is currently one of the moderators of the AGMA Gear Failure Analysis course.